Photoionization model for streamer propagation mode change in simulation model for streamers in dielectric liquids

To cite this article: I Madshaven *et al* 2020 *Plasma Res. Express* **2** 015002

View the article online for updates and enhancements.

Plasma Research Express

Photoionization model for streamer propagation mode change in simulation model for streamers in dielectric liquids

I Madshaven[1] , OL Hestad[2] , M Unge[3], O Hjortstam[3] and PO Åstrand[1,4]

[1] Department of Chemistry, NTNU—Norwegian University of Science and Technology, 7491 Trondheim, Norway
[2] SINTEF Energy Research, 7465 Trondheim, Norway
[3] ABB Corporate Research, 72178 Västerås, Sweden
[4] Author to whom any correspondence should be addressed.

E-mail: per-olof.aastrand@ntnu.no

Abstract

Radiation is important for the propagation of streamers in dielectric liquids. Photoionization is a possibility, but the effect is difficult to differentiate from other contributions. In this work, we model radiation from the streamer head, causing photoionization when absorbed in the liquid. We find that photoionization is local in space (μm-scale). The radiation absorption cross section is modeled considering that the ionization potential (IP) is dependent on the electric field. The result is a steep increase in the ionization rate when the electric field reduces the IP below the energy of the first electronically excited state, which is interpreted as a possible mechanism for changing from slow to fast streamers. By combining a simulation model for slow streamers based on the avalanche mechanism with a change to fast mode based on a photoionization threshold for the electric field, we demonstrate how the conductivity of the streamer channel can be important for switching between slow and fast streamer propagation modes.

1. Introduction

Dielectric liquids are widely used in high-voltage equipment, such as power transformers, because of their high electrical withstand strength and ability to act as a coolant [1]. If the electrical withstand strength of the liquid is exceeded, partial discharges followed by propagating discharges can occur and create prebreakdown channels called 'streamers'. Streamers are commonly classified by their polarity and propagation speed, ranging from below 0.1 kms^{-1} for the 1st mode to above 100 kms^{-1} for the 4th mode [2]. Streamers can be photographed by schlieren techniques, which captures the difference in permittivity between the gaseous streamer channel and the surrounding liquid [3], or by capturing light emitted by the streamer [4]. Continuous dim light has been observed from both the streamer channel and the streamer tip [5], as well as bright light from the streamer tip and re-illuminations of the streamer channel [5, 6]. The intensity of the emitted light and the occurrence of re-illuminations increases with higher streamer propagation modes. Photoionization by light absorbed in the liquid has been proposed as a possible feed-forward mechanism involved in the fast 3rd and 4th mode streamers [6, 7].

Streamer propagation is a multiscale, multiphysics phenomenon involving numerous mechanisms and processes [2]. Developing predictive models and simulations is challenging, but many attempts exist [8, 9]. Simulations have often focused on one aspect of the problem, such as the electric field [10, 11], production of free electrons ([12]), conductance of the streamer channels ([13]), inhomogeneities ([14]), or the plasma within the channels [15].

In this work we investigate a model for photoionization [16, 17] and combine it with a simulation model for propagation of streamers through an avalanche mechanism [18, 19]. The simplified cases studied in [16, 17], mimicking a streamer in a tube, can give only one streamer mode change. However, by not restricting the streamer to a 'tube' and including the dynamics of the streamer channel, we now demonstrate that the streamer

can change between slow and fast mode multiple times during a simulation. The present work is organized as follows: Theory on molecular energy states and radiation is given in the next section. The photoionization model is presented, evaluated and discussed in sections 3, 4 and 5, respectively. Section 6 describes the simulation model based on electron avalanches, with photoionization included, and the results of this model is presented in section 7. The model and the results are discussed in section 8, with the main conclusions summarized in section 9.

2. Molecular energy states and radiation

Molecules exist in quantum states with different energy $\mathcal{E}_n$. Excitation to a state of higher energy or relaxation to a state of lower energy can be achieved by absorbing or emitting a photon, respectively. The energy difference between molecular vibrational states is in the range meV to about 0.5 eV, while molecular electronic states have energies from some eV and up to around 20 eV. Change in vibrational states corresponds to infrared (IR) radiation (room temperature is about 25 meV), whereas visible (VIS) light (1.7–3.1 eV) and ultraviolet (UV) light (above 3.1 eV) normally correspond to electronic excitations. The transition probabilities to lower states gives the lifetime of an excited state, which varies from fs to several μs. In the case of fluorescence, an excited molecule relaxes through one or more states, before relaxing to the electronic ground state. The final relaxation is the most energetic and has the longest decay time, e.g. about 7.3 eV and 1 ns in liquid cyclohexane [20].

The ionization potential (IP) of a molecule is the energy required to excite an electron from the ground state $\mathcal{E}_0$ to an unbound state. Applying an external electric field $\boldsymbol{E}$ decreases the IP [21]

$$\mathcal{E}_{\mathrm{FDIP}}(E,\,\theta_e) = \mathcal{E}_{\mathrm{IP}} - \beta\cos\theta_e\,\sqrt{\frac{E}{\epsilon_r E_{a_0}}}\,, \tag{1}$$

where $\mathcal{E}_{\mathrm{IP}}$ is the zero-field IP, $E_{a_0} = 5.14 \times 10^{11}\,\mathrm{Vm}^{-1}$, ϵ_r is the relative permittivity of the liquid, $\cos\theta_e = \hat{\boldsymbol{k}}_e \cdot \hat{\boldsymbol{E}}$, and $\boldsymbol{k}_e$ is the momentum of emitted electron. The parameter $\beta = 54.4$ eV for the hydrogen atom, and similar values have been estimated for cyclohexane and several other molecules [21]. The energy of excited states is usually not significantly affected by the electric field in comparison to the field-dependence of the IP [21–23].

Spectral analysis of the light emitted from streamers show a broad band of photon energies up towards 3–4 eV [24, 25]. Distinct peaks in the emission spectrum reveal the presence of entities such as H_2, C_2, and CH_4, which are likely products of dissociation and recombination of hydrocarbon molecules from the base liquid [24, 26]. Stark broadening of the H_α-line can be investigated to find electron densities above $10^{24}\mathrm{m}^{-3}$, while the relation between the H_α and the H_β-line point to electron temperatures in the area of 10 kK [27]. Furthermore, rotational and vibrational temperatures of several kK can be estimated from spectral emission of C_2 Swan bands [28].

During a streamer breakdown, electrons (and other charged particles) are gaining energy and are accelerated in the electric field. Energy can be exchanged with other particles through collisions, possibly resulting in excitation, ionization or dissociation of molecules. Subsequently, relaxation or recombination can cause photon emission. The radiation B is absorbed by the medium, given by $\nabla B = -B\sigma\rho$ (Beer–Lambert law), where σ is the absorption cross section and ρ is the number density of the medium. Integration in spherical symmetry yields

$$\boldsymbol{B}(r) = \boldsymbol{B_0}\left(\frac{r_0}{r}\right)^2 \exp\left(-\int_{r_0}^{r} \rho\,\sigma\,\mathrm{d}\ell\right), \tag{2}$$

where $\boldsymbol{B}(r = r_0) = \boldsymbol{B_0} = B_0\hat{\boldsymbol{r}}$. The ionization cross section of cyclohexane, for instance, increases from close to zero below the IP to about 5×10^{-21} m^2 over the range of around 1 eV [29]. For single photons, cyclohexane begins to absorb around the first excitation energy and the absorption cross section increases steadily for higher photon energies [30]. A streamer could generate high-energy photons, which are rapidly absorbed by the liquid and therefore not measured by experiments [24].
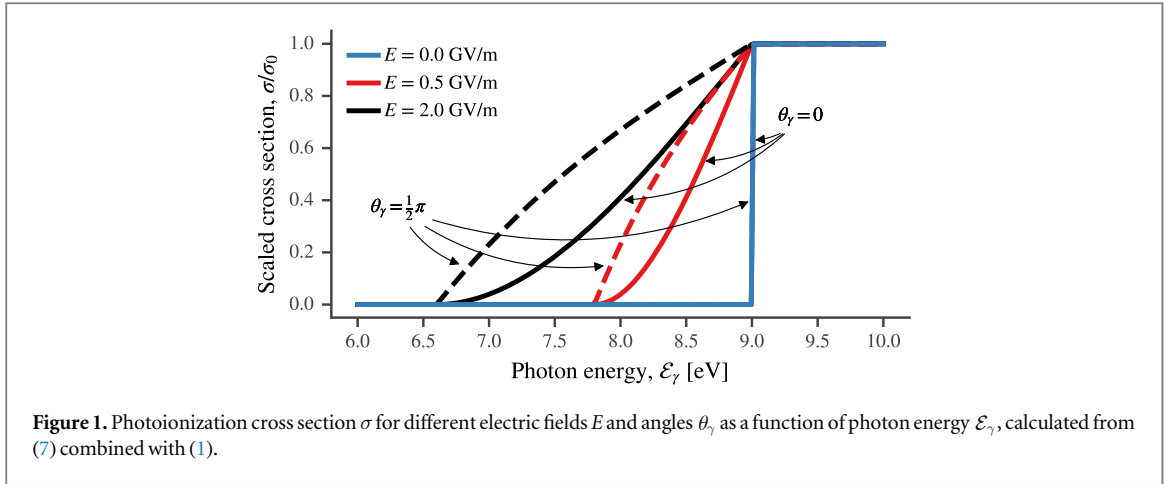
From the radiation B, the photon number density n_γ is given by [31]

$$n_\gamma = B/\mathcal{E}_\gamma c, \tag{3}$$

where $\mathcal{E}_\gamma$ is the photon energy and c is the speed of light in vacuum. From the Beer–Lambert law and (3) it follows that $\nabla n_\gamma = -n_\gamma\sigma\rho$. Generally, σ is a superposition of all (absorption) cross sections, however, when excitations can be neglected and only ionization is considered, the ionization rate W (per volume) is given by the change in n_γ,

$$W = -\partial_t n_\gamma = n_\gamma \sigma\rho c, \tag{4}$$

where we have used the continuity equation $\partial_t n_\gamma + \nabla(c n_\gamma) = 0$. Within a given volume $\mathcal{V}$, the rate of ionizing events is $W\mathcal{V}$ and the number of molecules is $\rho\mathcal{V}$, which gives the ionization rate per molecule

Figure 1. Photoionization cross section σ for different electric fields E and angles θ_γ as a function of photon energy $\mathcal{E}_\gamma$, calculated from (7) combined with (1).

$$w(r) = \frac{WV}{\rho V} = \int \frac{B(r, \mathcal{E}_\gamma)\, \sigma(r, \mathcal{E}_\gamma)}{\mathcal{E}_\gamma}\, d\mathcal{E}_\gamma, \qquad (5)$$

where we have explicitly stated the radiation and cross section as functions of the position r and the photon energy $\mathcal{E}_\gamma$. For instance, $w = 10^{-3}\ \mu$s implies that 0.1% of the molecules would be ionized within a μs.

3. Defining the streamer radiation model

Streamers can emit light sporadically from the channel (re-illuminations) and continuously from the streamer head, with fast streamers emitting more light than slow streamers [6]. In this work, we investigate the possibility of light emitted from the gaseous streamer head causing ionization in the liquid, resulting in a change to a faster streamer mode.

The probability of emitting the electron in a given direction is dependent on the momentum of the absorbed photon, i.e. the differential cross section $d\sigma$ is dependent on the differential solid angle $d\Omega$,

$$d\sigma \propto \sin^2\theta\, d\Omega, \qquad (6)$$

where $\cos\theta = \hat{\boldsymbol{k}}_e \cdot \hat{\boldsymbol{k}}_\gamma$. When $\mathcal{E}_\gamma < \mathcal{E}_{IP}$ we solve for $\mathcal{E}_\gamma = \mathcal{E}_{FDIP}(E, \Theta)$ in (1) to find the maximum possible angle Θ of electron emission. Then we integrate (6) over all angles where $\theta < \Theta$ to arrive at an expression for the photoionization cross section
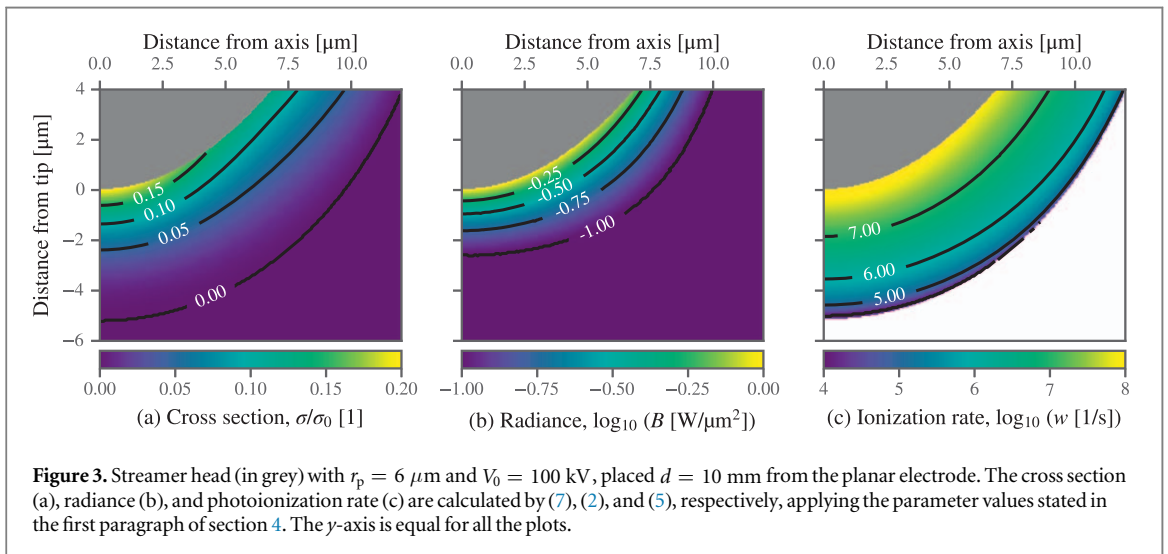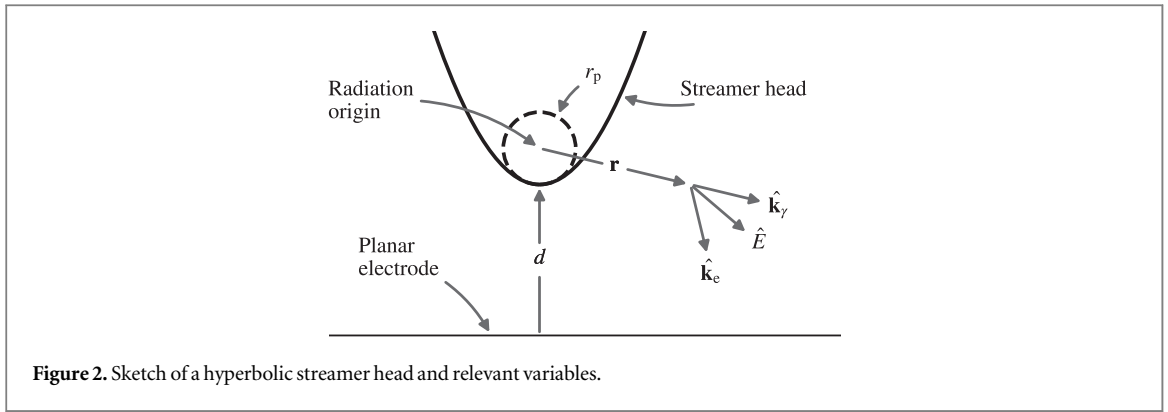
$$\sigma/\sigma_0 = 1 - \tfrac{1}{4}(1 + \cos^2\theta_\gamma)(3\cos\Theta - \cos^3\Theta)$$
$$- \tfrac{1}{2}\sin^2\theta_\gamma \cos^3\Theta, \qquad (7)$$

where $\cos\theta_\gamma = \hat{\boldsymbol{k}}_\gamma \cdot \hat{\boldsymbol{E}}$. Since (6) just gives a proportionality relation, (7) has been scaled such that $\sigma(\Theta = \tfrac{1}{2}\pi, \theta_\gamma) = \sigma_0$. This is illustrated by figure 1, where $\sigma = 0$ when $\mathcal{E}_\gamma < \mathcal{E}_{FDIP}$, $\sigma = \sigma_0$ when $\mathcal{E}_\gamma > \mathcal{E}_{IP}$, and dependent on $\boldsymbol{E}$ and $\boldsymbol{k}_\gamma$ when $\mathcal{E}_{FDIP} < \mathcal{E}_\gamma < \mathcal{E}_{IP}$. For example, for $\mathcal{E}_\gamma = 7.5$ eV and $E = 2GV\ m^{-1}$, we find $\Theta = 0.3\pi$, implying that $\mathcal{E}_{FDIP}(E, \theta_e < 0.3\pi) < \mathcal{E}_\gamma$. According to (6), photons with $\theta_\gamma = \tfrac{1}{2}\pi$ (perpendicular to $\boldsymbol{E}$) have a higher chance of emitting an electron in this region ($\theta_e < \Theta$) than photons with $\theta_\gamma = 0$. This is reflected in the different cross sections in figure 1.

We choose $z = (d + r_p)$ as the origin of radiation with a radiance $B(r = r_p) = B_0$, see figure 2. Generally, B_0 is comprised of a distribution of photon energies, however, we choose to limit the model to only consider radiation from a single low-energy excited state ($\mathcal{E}_\gamma = \mathcal{E}_n - \mathcal{E}_0$), since low-energy states are likely the most abundant ones. Radiation can cause ionization if the photon energy exceeds the field-dependent IP, i.e. $\mathcal{E}_\gamma > \mathcal{E}_{FDIP}$. Prolate spheroid coordinates are used to calculate the Laplacian electric field magnitude and direction [18], in order to calculate σ by (7). The radiance B in (2) and the ionization rate w in (5) can then be calculated, assuming low density ($\rho \approx 0$) within the streamer head and constant density in the liquid. The integration of σ is performed numerically in a straight line from $z = (d + r_p)$. Two-photon excitations (absorption to excited states) and scattering (absorption and re-emission) are assumed to have low influence and are ignored in this work.

4. Properties of the radiation model
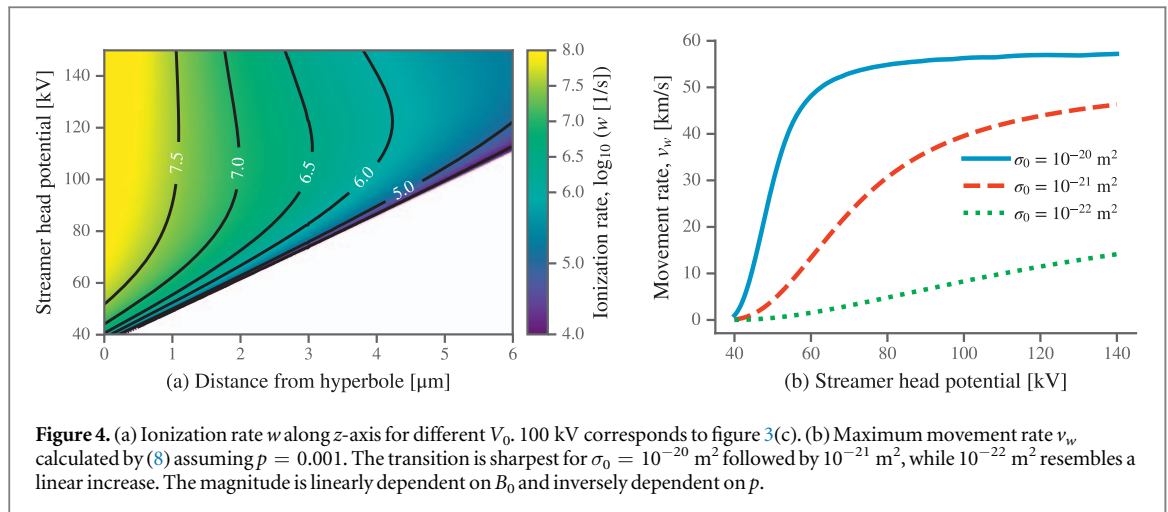
To evaluate the radiation model, a hyperbolic streamer head with tip curvature $r_p = 6\ \mu$m is placed with a gap $d = 10$ mm towards a planar electrode (see figure 2). The model liquid is similar to cyclohexane, assuming radiation from the lowest excited state, i.e. $\mathcal{E}_\gamma = \mathcal{E}_1 - \mathcal{E}_0 = 7$ eV, $\mathcal{E}_{IP} = 9$ eV, $\sigma_0 = 10^{-21}$ m^2 and

Figure 2. Sketch of a hyperbolic streamer head and relevant variables.

(a) Cross section, σ/σ_0 [1]   (b) Radiance, $\log_{10}(B\ [\text{W}/\mu\text{m}^2])$ (c) Ionization rate, $\log_{10}(w\ [1/\text{s}])$

Figure 3. Streamer head (in grey) with $r_p = 6\ \mu$m and $V_0 = 100$ kV, placed $d = 10$ mm from the planar electrode. The cross section (a), radiance (b), and photoionization rate (c) are calculated by (7), (2), and (5), respectively, applying the parameter values stated in the first paragraph of section 4. The y-axis is equal for all the plots.

$\rho = 5.6 \times 10^{27}/\text{m}^3$ [16]. The initial power of the radiation is set to $B_0 = 1\text{W}\ \mu\text{m}^{-2}$, which is in the range of the power needed to evaporate the liquid [32]. Several other factors, such as Joule heating, can contribute to evaporate the liquid, and the contribution from radiation is unknown. Furthermore, the actual radiation power of a streamer is unknown and likely to fluctuate. However, since the results are linear in B_0, setting a value enables a discussion of whether the results are reasonable.

The area where ionization is possible increases with V_0 and covers a range of about 5 μm from the streamer head when $V_0 = 100$ kV, see figure 3(a). At the z-axis, $\sin\theta_\gamma = 0$, the cross section σ is yet the largest close to the streamer head, because of the strong electric field E. Figure 3(a) shows how σ declines as the distance from the streamer head increases. One could expect that σ would decline fast close to the streamer head as the distance from the z-axis increases, since E declines, however, an increase in $\sin\theta_\gamma$ when moving away off-axis counteracts the reduction in E, resulting in just a slight decrease in σ. Numeric integration of σ in figure 3(a) is applied to find B in (2), see figure 3(b). The rapid decay of the radiance is expected considering that $\rho\sigma_0 = 5.6/\mu$m (i.e. a penetration depth of $\delta = 1/\sigma\rho = 0.18\ \mu$m) is included in the exponent in (2). The ionization rate per molecule w in (5) is presented in figure 3(c). A major finding is that photoionization is indeed a very local effect in dielectric liquids, mainly occurring within a few μm of the source, which is the streamer head in this case.

Increasing V_0 increases the ionization rate w close to the streamer head and increases the reach of the ionization zone in figure 4(a) up to about 100 kV. At higher potentials, the ionization rate at a distance of some μm decreases since much of the radiation is absorbed within the first μm. This is evident from the contour for $w = 10^6/\text{s}$, for instance. We may hypothesize that photoionization cause streamer propagation once a degree of ionization p is obtained. The time t_w required to reach p is $t_w = p/w$, and this time varies with the distance from the streamer head Δr. Both the time and the distance are important, obtaining p fast very close to the streamer have to be weighed against having a longer t_w at a distance further from the streamer. As such, we define the photoionization speed of the streamer,

Figure 4. (a) Ionization rate w along z-axis for different V_0. 100 kV corresponds to figure 3(c). (b) Maximum movement rate v_w calculated by (8) assuming $p = 0.001$. The transition is sharpest for $\sigma_0 = 10^{-20}$ m^2 followed by 10^{-21} m^2, while 10^{-22} m^2 resembles a linear increase. The magnitude is linearly dependent on B_0 and inversely dependent on p.

$$v_w = \max\left\{\frac{\Delta r}{t_w}\right\} = \max\left\{\frac{\Delta r w}{p}\right\}. \tag{8}$$

The speed v_w is set to the maximum value of the product of Δr and w, where $w = w(\Delta r)$ is calculated numerically, for a range of Δr close to the streamer head. Since measured electron densities in streamers point to a degree of ionization in the range of 0.1% to 1% [27, 28], we assume that $p = 0.001$ is required for propagation. The photoionization speed v_w of the data in figure 4(a) is presented in figure 4(b), showing an increase in v_w as $\mathcal{E}_{\text{FDIP}}$ is reduced below $\mathcal{E}_\gamma$. Changing to $p = 0.01$ would yield the same result if also B was increased tenfold since the magnitude of v_w is dependent on the radiated power ($v_w \propto w \propto B_0$). Neither the value of B_0 or p is known and we cannot assert that photoionization indeed leads to such a drastic speed increase v_w as shown in figure 4(b), however, the important part of the model is to show that photoionization can be affected by the electric field strength and that the effect is local. Physically, when the liquid no longer can absorb light to a bound excited state, the result is direct ionization, and it is reasonable that ionization contributes more to the propagation speed than emission of light or local heating. The transition from low to high speed (low to high ionization rate) in figure 4(b) for the largest cross section ($\sigma_0 = 10^{-20}$m^2) occurs over a short voltage range of about 20 kV.

5. Discussion of the radiation model

The modeled photoionization cross section increased from zero towards a maximum of 10^{-21} m^2, which resulted in rapid absorption within a few μm. The real absorption might be even more rapid, since the cross section of cyclohexane is about 5 times larger for ionizing radiation [29]. An increase in the cross section to $\sigma_0 = 5 \times 10^{-21}$ m^2 gives a shorter penetration depth $\delta = 1/\sigma\rho$, which results in even shorter range for the radiance and ionization than shown in figure 3. According to figure 4(b) this gives a steep increase in the movement rate v_w. The fluorescence of cyclohexane is consistent with radiation from the first excited state [20], but the absorption to this state is intrinsically low [30]. Radiation from fluorescence may thus transport energy away from the streamer head.

Excited molecules in the liquid have a high probability of non-radiative relaxation which heats the liquid. In strong electric fields, the IP is reduced and bound excited states become unbound, i.e. they appear above the ionization threshold [22], and instead of heating, absorption causes ionization. It is, however, difficult to assess how an electric field affects cross sections. By assuming an increase in the cross section when the field is increased (see figure 1), more radiation is absorbed, but the effect also becomes more local. The model therefore predicts a faster propagation when the radiation from the streamer head is absorbed directly in front of the streamer, in line with figure 4(b) where higher cross sections results in higher speeds.

The photoionization cross sections σ for linear alkanes and aromatics differ by more than a decade, from about 1×10^{-22} m^2 to 5×10^{-21} m^2 [33]. Given a number density $\rho = 5 \times 10^{27}/$ m^3, the penetration depth δ is between 2 μm and 0.04 μm, respectively. Ionizing radiation emitted when electrons recombine with cations is therefore rapidly absorbed, however, non-ionizing radiation having lower absorption cross section can propagate further. If we assume that fluorescent radiation from cyclohexane is absorbed with a cross section of 1/100 of the ionizing radiation, this radiation has a reach of several μm. In combination with a low-IP aromatic additive, having a larger cross section, the reach of the radiation is reduced, but radiation absorbed by the additive causes ionization whereas absorption to cyclohexane results in heat. For instance, pyrene ($\mathcal{E}_{\text{IP}} = 7$ eV [23]) is ionized when absorbing fluorescent radiation from cyclohexane, and could facilitate streamer growth by

providing seed electrons for new avalanches. A similar result is found for gases where additives absorbing ionizing radiation can increase the streamer propagation speed for a single branch [34]. Furthermore, excited states of the additives can have lifetimes of tens to hundreds of ns [35], which increases the probability of two-photon ionization compared with a lifetimes up to about a ns in pure cyclohexane [20]. As such, low-IP additives can facilitate slow streamers by reducing the inception voltage, increase the propagation length, and reduce the breakdown voltage [36]. Facilitated growth can lead to more branching, which is possibly why such additives can increase the acceleration voltage [36]. Increased branching can stabilize the streamer through electrostatic shielding, however, photoionization in front of the streamer can be involved in a change to a fast mode [6, 7]. For instance, if one branch escapes the shielding from the others, the electric field surrounding it would increase, reducing the IP and allowing more of the radiation to cause ionization.

Under normal conditions, electrical insulation in liquids is a steady-state process where the added energy by the applied electrostatic potential is released through radiation as either heat or light in the UV/VIS region. Similarly, during a streamer breakdown, the added energy can dissipate in the liquid, but also cause streamer propagation when the energy dissipation is concentrated. The availability of electronic excited states is therefore crucial, and because of the strong field-dependence of the IP, the number of available excited states decrease with increasing field [22]. Additives with lower excitation energies, sustaining to higher fields, may therefore be an approach to increase the acceleration voltage, as indicated experimentally [37, 38]. The available excited states and absorption probabilities are therefore important to consider. One additive that has been studied [36], pyrene, has excited states between 4 and 7 eV (in gas) [23] and can thus absorb and radiate energy which is generally not absorbed by cyclohexane. Pyrene and dimethylaniline (DMA) have a similar $\mathcal{E}_{IP}$ and first excitation energy, and both additives increase the acceleration voltage in cyclohexane [36, 39]. However, whereas pyrene absorbs radiation at the lowest excitation energy which is a π to π^* transition, the lowest excited state of DMA is non-absorbing [40] and thus the second lowest excitation energy should be considered instead. This increases the excitation energy from 4 to 5 eV [40]. It is not uncommon that the lowest state is non-absorbing. For example in azobenzenes, also studied as an additive in streamer experiments [37], the lowest n to π^* transition is non-absorbing, whereas the second excitation, π to π^*, has a high absorbance and gives the molecules their color [41]. Excited states most likely play a role both in collision events with primary electrons (affecting impact ionization) and in absorption of light (affecting photoionization), but the different contributions are difficult to disentangle from other mechanisms. In the end, which effects that are significant under realistic conditions need to be established by cleverly designed experiments.

There is a relatively small number of electronic states available below the IP, but a large number of states above the IP, often considered as a continuum. This makes the cross section for ionization larger than the cross section for absorption to a bound excited state. Consequently, as the IP decreases with an increase in the electric field, the cross section at certain energies increases. A local electric field in excess of 0.5 GV m^{-1} is sufficient to remove all excited states of cyclohexane in gas phase [22]. In a liquid where $\epsilon_r = 2$, we find that a local field of 1.4 GV m^{-1} reduce the IP by 2 eV from (1), which is sufficient to reduce $\mathcal{E}_{FDIP}$ below the first excited state in cyclohexane. When the electric field is above this threshold, cyclohexane cannot absorb radiation to a bound state and is ionized instead. For a hyperbolic streamer head with $r_p = 6$ μm in a gap $d = 10$ mm, this threshold is reached at a potential of 37 kV, assuming that the local field is the same as the macroscopic field, and the transition in speed occurs above this in figure 4(b). The threshold is close to the acceleration voltage in a tube [42], but much lower than the acceleration voltage in a non-constricted large gap [36]. However, the actual tip radius of the streamer and the degree of branching are important when calculating the tip field, as well as space charge generated in the liquid. Furthermore, the local field can differ from the macroscopic field. For instance, the field is increased by a factor of 1.3 in a spherical cavity in a non-polar liquid [21]. The model mainly demonstrates how rapid ionizing radiation (high cross section) is absorbed in the liquid.

6. Avalanche model with photoionization

In earlier work we have developed a model for simulating the propagation of positive streamers in non-polar liquids through an electron avalanche mechanism [18, 19]. Here we incorporate the photoionization mechanism into the streamer model. A short overview of the model is given below.

Simulation parameters are similar with those used in our previous works [18, 19], i.e. a needle-plane gap with cyclohexane as a model liquid. The needle is represented by a hyperbole (see figure 2) with tip curvature $r_n = 6.0$ μm, placed $d = 10$ mm above a grounded plane. The potential V_0 applied to the needle gives rise to an electric field **E** in the gap. The Laplacian electric field is calculated analytically in prolate spheroid coordinates. Electrons detach from anions in the liquid (assumed ion density $n_{ion} = 2 \times 10^{12}$ m^{-3}) and grow into electron avalanches if the field is sufficiently strong. The number of electrons N_e in an avalanche is given by

$$\ln N_{\mathrm{e}} = \sum_i E_i \, \mu_{\mathrm{e}} \, \alpha_{\mathrm{m}} \, e^{-E_\alpha / E_i} \Delta t, \tag{9}$$

where $\alpha_{\mathrm{m}} = 130 \, /\mu\mathrm{m}$ and $E_\alpha = 1.9\mathrm{GV}$, m^{-1} for cyclohexane [43], $\mu_{\mathrm{e}} = 45 \, \mathrm{mm}^2\mathrm{Vs}^{-1}$ is the electron mobility, i denotes a simulation iteration, and $\Delta t = 1$ ps is the time step. If an avalanche obtains a number of electrons $N_{\mathrm{e}} > 10^{10}$, it is considered 'critical'. The streamer grows by placing a new streamer head wherever an avalanche becomes critical. Each streamer head, an extremity of the streamer, is represented by a hyperbole with tip curvature $r_{\mathrm{s}} = 6.0 \, \mu\mathrm{m}$. After the inception of the streamer, the electric potential V and the electric field $\boldsymbol{E}$ for a given position $\boldsymbol{r}$ is calculated by a superposition of the needle and all the streamer heads,

$$V(\boldsymbol{r}) = \sum_i k_i V_i(\boldsymbol{r}), \quad \boldsymbol{E}(\boldsymbol{r}) = \sum_i k_i \boldsymbol{E}_i(\boldsymbol{r}), \tag{10}$$

where i denotes a streamer head. The coefficients k_i correct for electrostatic shielding between the heads. Whenever a new head is added, the streamer structure is optimized, possibly removing one or more existing heads. Streamer heads within 50 μm of another head closer to the plane, and heads with $k_i < 0.1$, are removed [18].

Each streamer head is associated with a resistance in the channel towards the needle and a capacitance in the gap towards the planar electrode [19]. The resistance R and capacitance C is given by

$$R \propto \ell, \;\; \text{and } C \propto \left(\ln \frac{4z + 2r_{\mathrm{s}}}{r_{\mathrm{s}}} \right)^{-1}, \tag{11}$$

where ℓ is the distance from the needle to the streamer head and z is the position of the streamer head in the gap. New streamer heads are given a potential which magnitude depends on their position as well as the configuration of the streamer. The potential V_i of each streamer head is relaxed towards the potential of the needle electrode V_0 each simulation time step. This is achieved by reducing the difference in potential,

$$\Delta V_i = V_0 - V_i \;\rightarrow\; V_i = V_0 - \Delta V_i e^{-\Delta t / \tau_i}, \tag{12}$$

where the time constant is given by $\tau = \tau_0 RC$ and $\tau_0 = 1 \, \mu$s. If the electric field within the streamer channel $E_{\mathrm{s}} = \Delta V_i / \ell_i$ exceeds a threshold E_{bd}, a breakdown in the channel occurs, equalizing the potential of the streamer head and the needle. A channel breakdown affects the potential of a single streamer head since each streamer head is 'individually' connected to the needle [19].

Calculating the photoionization cross section in (7) is a computational expensive operation, contrary to our avalanche simulation model which is intended to be relatively simple and computationally efficient. The photoionization model indicates an increase in speed (see figure 4) when $\mathcal{E}_{\mathrm{FDIP}} < \mathcal{E}_n$ over a short distance into the liquid. To model photoionization in an efficient way, we add a 'photoionization speed' v_w to each streamer head exceeding a threshold $E_w = 3.1\mathrm{GV} \, \mathrm{m}^{-1}$. This is implemented by moving such streamer heads a distance $\boldsymbol{s}_w = v_w \Delta t \, \hat{\boldsymbol{z}}$. Equation (8) predicts a speed v_w given a set of parameter values (see figure 4(b)), where some, such as radiation power and degree of ionization, are unknown. The chosen power of 1W $\mu\mathrm{m}^{-2}$ exceeds 100 W in total when distributed over a streamer head with a radius of some μm. Since a streamer requires about 5 mJ/m for propagation [32], the expected speed exceeds 20km s^{-1}, which is in line with figure 4(b). We choose $v_w = 20$km s^{-1} for the simulations, which is the order of magnitude given by figure 4(b), but slow compared to some 4th mode streamers exceeding 100km s^{-1}. However, this is sufficient to investigate transitions between slow and fast mode since it is more than an order of magnitude above the speed predicted by the simulations without a photoionization contribution [18].

7. Results from avalanche model with photoionization

For evaluating the model we investigate the influence of the applied voltage V_0 (square wave), the threshold for breakdown in the channel E_{bd}, while excluding or including photoionization. Figure 5 illustrates the behavior of two different single head streamers. Streamer 1 starts in a fast mode, but after propagating some mm the electric field at the streamer head has dropped below the threshold for fast propagation E_w and the streamer changes to a slower mode of propagation. Streamer 2 starts in a slow mode, but having no potential drop within the streamer channel, the electric field at the streamer head increases during propagation and the streamer changes to a fast mode for the final few mm of the gap.

Both streamer 1 and 2 in figure 5 are simplified cases with a single head and a constant E_{s}, however, the simulations in figure 6(a) show a similar behavior, but at higher voltages. In the simulations with low E_{bd}, resulting in a low E_{s}, the streamers switch to fast mode for the final portion of the gap, and the portion increases with increasing voltage. According to figure 5, all of the streamers in figure 6(a) starts above the threshold of $E_w = 3.1\mathrm{GV} \, \mathrm{m}^{-1}$, however, as the streamer propagates and more streamer heads are added, electrostatic shielding between the heads quickly reduces the electric field below this threshold. Increasing E_{bd} gives an on average higher E_{s} and figure 6(a) illustrates how this can make streamers change between fast and slow propagation.

Figure 5. Electric field strength at the tip of an electric hyperboloid with a tip curvature of 6.0 μm for a given position and potential. The dotted white lines show the electric field thresholds for IP reduction by 2 eV (1.4 GV m^{-1}) and 3 eV (E_w = 3.1 GV m^{-1}), as well as E_α = 1.9 GV m^{-1}. The dashed gray lines represent streamers. (1) indicate how an electric field of E_s = 4 kV mm^{-1} can change the propagation mode from fast to slow in the beginning of the gap. (2) indicate how a highly conducting streamer can change from slow to fast towards the end of the gap.

Figure 6. (a) Streak plots showing the position of the leading streamer head as a function of time. The transition from slow to fast or from fast to slow is dependent on the needle potential and the channel breakdown threshold. (b) Propagation time and leading head potential, each as a function of leading head position in the gap, for V_0 = 110 kV and E_{bd} = 4 kV mm^{-1} in (a). The above data is generated by sampling the position and potential of the leading streamer head (closest to the opposing electrode) for every 10 μm of propagation of each simulation.
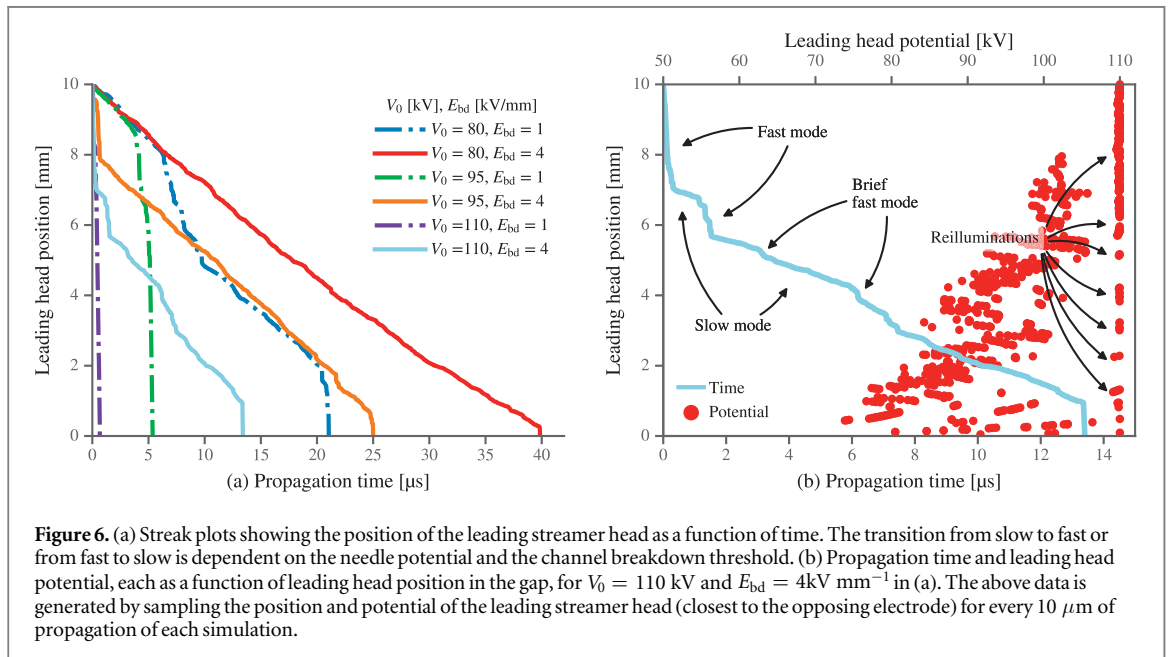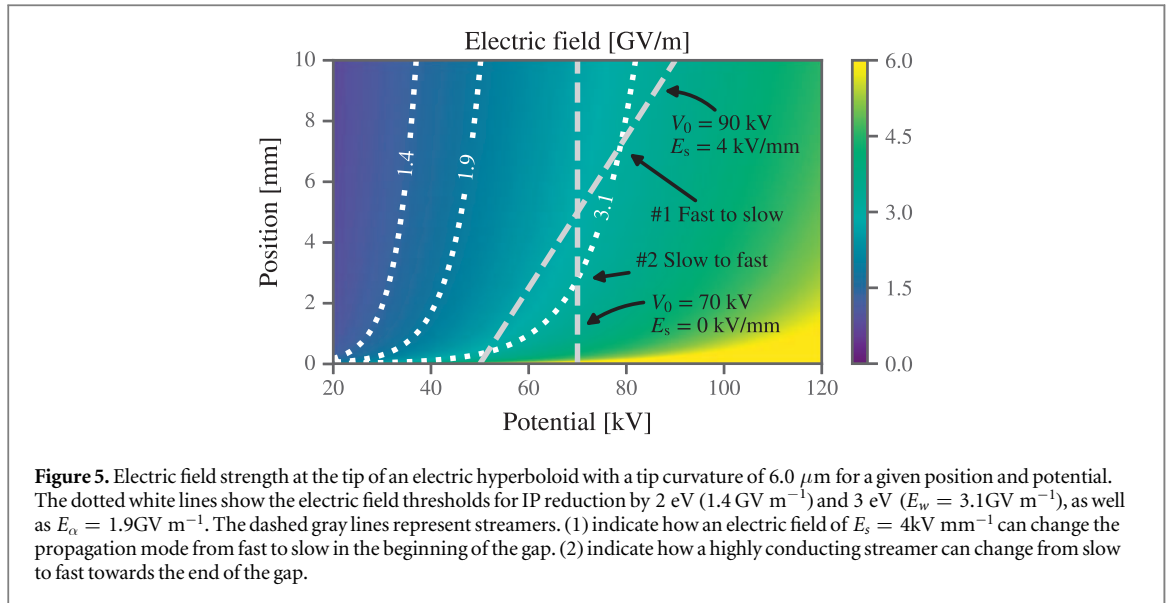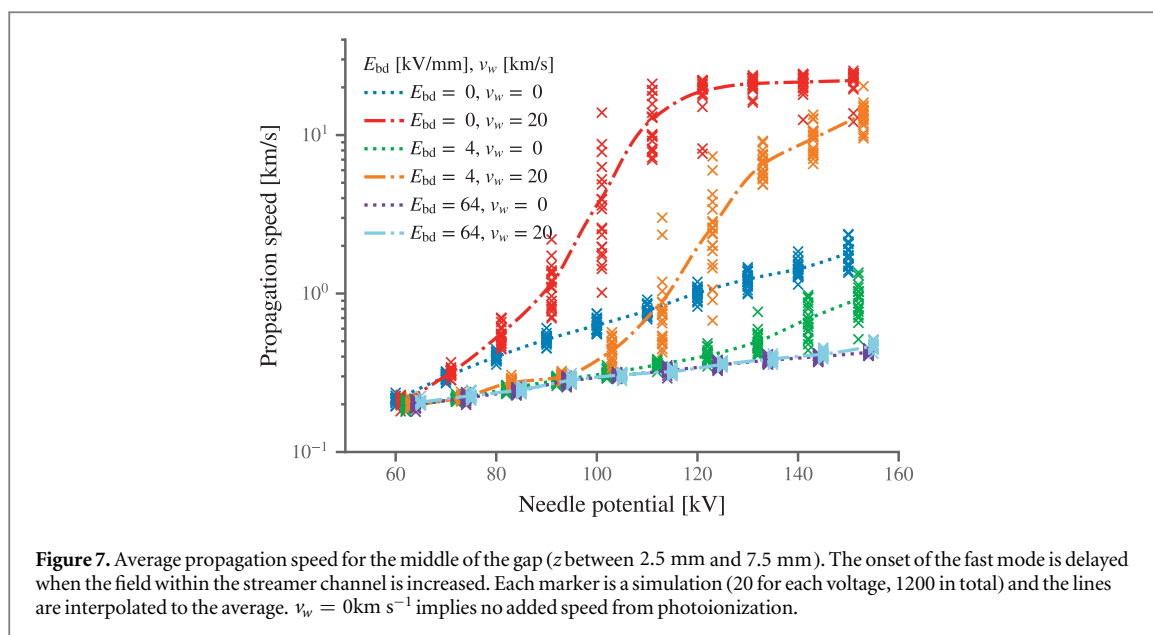
Figure 6(b) details a streamer beginning in fast mode and changing to slow propagation mode. Propagation reduces the potential at the streamer head. When the electric field at the tip is sufficiently reduced, the streamer changes to a slow mode. Re-illuminations, breakdowns within the streamer channel, sporadically increases the potential and can push the streamer over in a fast mode, however, often this 'fast mode' is brief and difficult to notice.

By considering a wider range of voltages in figure 7, the transition from slow to fast mode occurs at about 100 kV for a highly conducting streamer. Increasing E_{bd} decreases the average (in time) electric field at the streamer heads and thus delays the onset of the fast mode to about 120 kV. An acceleration voltage of 120 kV is consistent with longer gaps [36, 39], while for shorter gaps (5 mm) about 60 kV has been found [42]. As mentioned in our previous work, the propagation voltage predicted by the simulations is somewhat high compared with experiments, whereas the propagation speed is low for second mode streamers [18]. The present work does not aim to improve on these limitations for slow streamers, but rather demonstrate how changes between slow and fast propagation can occur in different parts of the gap. The propagation speed for slow-mode streamers is about ten times of that predicted by figure 7, but the difference can be removed by assuming a higher electron mobility or a higher seed density [18].

Figure 7. Average propagation speed for the middle of the gap (*z* between 2.5 mm and 7.5 mm). The onset of the fast mode is delayed when the field within the streamer channel is increased. Each marker is a simulation (20 for each voltage, 1200 in total) and the lines are interpolated to the average. $v_w = 0\,\text{km s}^{-1}$ implies no added speed from photoionization.

8. Discussion

The role of photoionization during discharge in liquids is difficult to assess. For breakdown in gases, ionizing radiation can penetrate far into the medium, providing seed electrons for avalanches. While similar reasoning have been suggested for liquids, we argue that, given the higher density of the liquid and the large cross section for ionizing radiation, the penetration depth is short and photoionization occurs locally. Which radiation energies that are ionizing and where they can cause direct ionization are dependent on the electric field, given the field-dependence of the IP as well as the ionization cross-section. Non-ionizing, low-energy radiation have longer range and can provide seed electrons through a two-step ionization process. However, ionization of impurities or additives are far more likely, especially when the radiation from the base liquid can ionize them directly or they have long-lived excited states.

Assuming that increasing the applied potential increases the amount of radiation, it also increases generation of seed electrons for avalanches. Seeds likely facilitates both propagation speed and branching, while electrostatic shielding between branches can regulate the propagation speed. One hypothesis is that the change to a fast mode occurs when one fast branch escapes the electrostatic shielding from the others. If the radiation from such a branch can penetrate deep into the liquid, energy is transported away from the streamer head, while new seeds and subsequent avalanches can result in electrostatic shielding. Both of these mechanisms can reduce the speed. However, we have presented a model where a strong electric field makes photoionization more localized, suppressing energy transport and branching. This can explain how a streamer changes to a fast propagation mode when the electric field is sufficiently strong.

The model is limited in the sense that we do not know the actual value for the radiated power (or its energy distribution) or the degree of ionization it takes for a streamer to propagate. To assess the model we chose a value for the radiated power, and showed that this would be sufficient to ionize the liquid at a reasonable rate. Whether obtaining this radiated power is feasible remains unknown.

9. Conclusion

Emission and absorption of light is important for streamer propagation. Radiation can transport energy away from the streamer as heat or create free electrons through ionization, however, ionizing radiation is rapidly absorbed and thus unlikely to create seed electrons at some distance from the streamer head. Furthermore, since increasing the electric field reduces the ionization potential, it also increases the ionization cross section, making photoionization a local process. The model based on the electron avalanche mechanism in combination with modeling photoionization close to the steamer tip is found to capture the feature of acceleration of the streamer tip above a critical voltage. The photoionization model is missing a proper estimation of the spectral intensity of the radiation as well as the resulting speed, and this need to be investigated in the future. Radiation and photoionization is often mentioned in streamer literature, however, the potential short reach of the ionizing radiation is an important aspect to consider in understanding streamers in dielectric liquids.

Acknowledgments

ORCID iDs

I Madshaven ⬤ https://orcid.org/0000-0002-2443-7448
OL Hestad ⬤ https://orcid.org/0000-0001-7585-1326
PO Åstrand ⬤ https://orcid.org/0000-0003-3384-7585

References

[1] Wedin P 2014 Electrical breakdown in dielectric liquids—a short overview *IEEE Electr Insul Mag* **30** 20–5

[2] Lesaint O 2016 Prebreakdown phenomena in liquids: propagation 'modes' and basic physical properties *J Phys. D: Appl. Phys.* **49** 144001

[3] Farazmand B 1961 Study of electric breakdown of liquid dielectrics using Schlieren optical techniques *Br. J. Appl. Phys.* **12** 251–4

[4] Sakamoto S and Yamada H 1980 Optical study of conduction and breakdown in dielectric liquids *IEEE Trans. Electr. Insul.* **EI-15** 171–81

[5] Dung N V, Høidalen H K, Linhjell D, Lundgaard L E and Unge M 2013 Effects of reduced pressure and additives on streamers in white oil in long point-plane gap *J Phys. D: Appl. Phys.* **46** 255501

[6] Linhjell D, Lundgaard L and Berg G 1994 Streamer propagation under impulse voltage in long point-plane oil gaps *IEEE Trans. Dielectr. Electr. Insul.* **1** 447–58

[7] Lundgaard L, Linhjell D, Berg G and Sigmond S 1998 Propagation of positive and negative streamers in oil with and without pressboard interfaces *IEEE Trans. Dielectr. Electr. Insul.* **5** 388–95

[8] Biller P 1996 A simple qualitative model for the different types of streamers in dielectric liquids *ICDL'96 12th Int. Conf. Conduct Break Dielectr Liq.* 189–92 IEEE.

[9] Beroual A 2016 Pre-breakdown mechanisms in dielectric liquids and predicting models *2016 IEEE Electr. Insul. Conf.* 117–28

[10] Niemeyer L, Pietronero L and Wiesmann H J 1984 Fractal dimension of dielectric breakdown *Phys. Rev. Lett.* **52** 1033–6

[11] Fofana I and Beroual A 1998 Predischarge models in dielectric liquids *Jpn. J. Appl. Phys.* **37** 2540–7

[12] Kim M, Hebner R and Hallock G 2008 Modeling the growth of streamers during liquid breakdown *IEEE Trans. Dielectr. Electr. Insul.* **15** 547–53

[13] Kupershtokh A L and Karpov D I 2006 Simulation of the development of branching streamer structures in dielectric liquids with pulsed conductivity of channels *Tech. Phys. Lett.* **32** 406–9

[14] Jadidian J, Zahn M, Lavesson N, Widlund O and Borg K 2014 Abrupt changes in streamer propagation velocity driven by electron velocity saturation and microscopic inhomogeneities *IEEE Trans. Plasma Sci.* **42** 1216–23

[15] Naidis G V 2016 Modelling the dynamics of plasma in gaseous channels during streamer propagation in hydrocarbon liquids *J Phys. D: Appl. Phys.* **49** 235208

[16] Madshaven I, Smalø H S, Unge M and Hestad O L 2016 Photoionization model for the transition to fast mode streamers in dielectric liquids *In 2016 IEEE Conf. Electr. Insul. Dielectr Phenom.* 400–3

[17] Madshaven I, Åstrand P O, Hestad O L, Unge M and Hjortstam O 2017 Modeling the transition to fast mode streamers in dielectric liquids *In 2017 IEEE 19th Int. Conf. Dielectr Liq.* 1–4

[18] Madshaven I, Åstrand P O, Hestad O L, Ingebrigtsen S, Unge M and Hjortstam O 2018 Simulation model for the propagation of second mode streamers in dielectric liquids using the Townsend-Meek criterion *J Phys. Commun.* **2** 105007

[19] Madshaven I, Hestad O L, Unge M, Hjortstam O and Åstrand P O 2019 Conductivity and capacitance of streamers in avalanche model for streamer propagation in dielectric liquids *Plasma Res. Express* **1** 035014

[20] Wickramaaratchi M A, Preses J M, Holroyd R A and Weston R E 1985 The lifetime of the fluorescent excited state in solid, liquid, and vapor phase cyclohexane *J Chem. Phys.* **82** 4745–52

[21] Smalø H S, Hestad O L, Ingebrigtsen S and Åstrand P O 2011 Field dependence on the molecular ionization potential and excitation energies compared to conductivity models for insulation materials at high electric fields *J Appl. Phys.* **109** 073306

[22] Davari N, Åstrand P O, Ingebrigtsen S and Unge M 2013 Excitation energies and ionization potentials at high electric fields for molecules relevant for electrically insulating liquids *J Appl. Phys.* **113** 143707

[23] Davari N, Åstrand P O and Unge M 2015 Density-functional calculations of field-dependent ionization potentials and excitation energies of aromatic molecules *Chem. Phys.* **447** 22–9

[24] Wong P and Forster E 1982 The dynamics of electrical breakdown in liquid hydrocarbons *IEEE Trans. Electr. Insul.* **EI-17** 203–20

[25] Bonifaci N and Denat A 1991 Spectral analysis of light emitted by prebreakdown phenomena in non-polar liquids and gases *IEEE Trans. Electr. Insul.* **26** 610–4

[26] Beroual A 1993 Electronic and gaseous processes in the prebreakdown phenomena of dielectric liquids *J Appl. Phys.* **73** 4528–33

[27] Bårmann P, Kröll S and Sunesson A 1996 Spectroscopic measurements of streamer filaments in electric breakdown in a dielectric liquid *J Phys. D: Appl. Phys.* **29** 1188–96

[28] Ingebrigtsen S, Bonifaci N, Denat A and Lesaint O 2008 Spectral analysis of the light emitted from streamers in chlorinated alkane and alkene liquids *J Phys. D: Appl. Phys.* **41** 235204

[29] Cool T A, Wang J, Nakajima K, Taatjes C A and Mcllroy A 2005 Photoionization cross sections for reaction intermediates in hydrocarbon combustion *Int. J. Mass. Spectrom.* **247** 18–27

[30] Jung J and Gress H 2003 Single-photon absorption of liquid cyclohexane, 2,2,4 trimethylpentane and tetramethylsilane in the vacuum ultraviolet *Chem. Phys. Lett.* **377** 495–500

[31] Carroll B W and Ostlie D A 2007 *An Introduction to Modern Astrophysics* 2nd edn. (San Francisco: Pearson Education)

[32] Gournay P and Lesaint O 1994 On the gaseous nature of positive filamentary streamers in hydrocarbon liquids. II: propagation, growth and collapse of gaseous filaments in pentane *J Phys. D: Appl. Phys.* **27** 2117–27

[33] Eschner M S and Zimmermann R 2011 Determination of photoionization cross-sections of different organic molecules using gas chromatography coupled to single-photon ionization (SPI) time-of-flight mass spectrometry (TOF-MS) with an electron-beam-pumped rare gas excimer light source (EBEL) *Appl. Spectrosc.* **65** 806–16

[34] Naidis G V 2018 Effects of photoionization characteristics on parameters of positive streamers *Plasma Res. Express* **1** 017001

[35] Brownrigg J T and Kenny J E 2009 Fluorescence intensities and lifetimes of aromatic hydrocarbons in cyclohexane solution: evidence of contact charge-transfer interactions with oxygen *J Phys. Chem.* A **113** 1049–59

[36] Lesaint O and Jung M 2000 On the relationship between streamer branching and propagation in liquids: influence of pyrene in cyclohexane *J Phys. D: Appl. Phys.* **33** 1360–8

[37] Unge M, Singha S, Dung N V, Linhjell D, Ingebrigtsen S and Lundgaard L E 2013 Enhancements in the lightning impulse breakdown characteristics of natural ester dielectric liquids *Appl. Phys. Lett.* **102** 172905

[38] Liang S, Wang F, Huang Z, Chen W, Wang Y and Li J 2019 Significantly improved electrical breakdown strength of natural ester liquid dielectrics by doping ultraviolet absorbing molecules *IEEE Access* **7** 73448–54

[39] Linhjell D, Ingebrigtsen S, Lundgaard L and Unge M 2011 Streamers in long point-plane gaps in cyclohexane with and without additives under step voltage *In 2011 IEEE Int Conf Dielectr Liq* 1–5

[40] Galván I F, Martín M E, Muñoz-Losa A and Aguilar M A 2009 Solvatochromic shifts on absorption and fluorescence bands of N,N-dimethylaniline *J Chem. Theory Comput.* **5** 341–9

[41] Åstrand P O, Ramanujam P S, Hvilsted S, Bak K L and Sauer S P A 2000 *Ab initio* calculation of the electronic spectrum of azobenzene dyes and its impact on the design of optical data storage materials *J. Am. Chem. Soc.* **122** 3482–7

[42] Linhjell D, Ingebrigtsen S, Lundgaard L and Unge M 2013 Positive breakdown streamers and acceleration in a small point-plane liquid gap and their variation with liquid properties *In Proc. Nord Insul. Symp.* 191–6

[43] Naidis G V 2015 On streamer inception in hydrocarbon liquids in point-plane gaps *IEEE Trans. Dielectr Electr. Insul.* **22** 2428–32